Contribution from the Department of Pharmaceutical Sciences, Nagoya City University, Nagoya 467, Japan, and Faculty of Pharmaceutical Sciences, University of Tokyo, Tokyo 113, Japan

Spectrophotometric and Resonance Raman Studies on the Formation of Phenolate and Thiolate Complexes of (Octaethylporphinato)iron(III)

Tadayuki Uno,*[1a] Keiichiro Hatano,[1a] Yoshifumi Nishimura,[1b] and Yoji Arata[1b]

Received July 28, 1989

Reactions of (octaethylporphinato)iron(III) methoxide, Fe(OEP)(OMe), with a series of phenols, carboxylic acids (ROH), and thiols (RSH) were monitored by spectrophotometric techniques. The equilibrium constants for addition of ROH to Fe(OEP)(OMe) were measured, and it was found that increased acidity of the ROH moiety caused the equilibrium constant to increase. The reaction of Fe(OEP)(OMe) with RSH proceeded significantly slowly at 20 °C. The second-order rate constants were obtained and were found to increase with the increase of RSH acidity. These indicate that dissociation of a proton from an ROH or RSH moiety will promote the formation of the product species Fe(OEP)(OR) or Fe(OEP)(SR). By the use of resonance Raman spectroscopy, both product species were found to be five-coordinate ferric high-spin complexes. The Fe(OEP)(OPh) complex showed the ν(Fe–OPh) stretching Raman line at 607 cm^{-1}. The visible absorption maxima of the porphyrin π to iron d_π transitions (CT band) of Fe(OEP)(OR) and Fe(OEP)(SR) were a linear function of the pK_a of ROH and RSH, and the hypsochromic shift with the increasing pK_a was explained in terms of the electron-donating ability of the OR and SR ligands. The absorption maxima of Fe(OEP)(SR) were generally shifted to longer wavelength than those of Fe(OEP)(OR).

Introduction

Cytochrome P-450 belongs to the monoxygenase class of enzymes and is the essential component of the metabolic transformation reactions in living organisms. The oxidizing intermediate of cytochrome P-450 has been assumed to be an iron(IV)–oxo porphyrin π cation radical,[2] an analogical intermediate known as compound I of the peroxidases.[3] Catalase occurs in almost all aerobically respiring organisms and serves to protect cells from the toxic effects of hydrogen peroxide. The reactions of catalase with hydroperoxides lead to the formation of an intermediate complex, which is also called compound I.[4] Although there are few spectroscopic data[5] available for catalase compound I, probably because of its instability, a similar iron(IV) porphyrin π-cation-radical structure has been proposed as the spectral analogue of cobalt porphyrin π cation radicals.[6]

The high-valent irons in these intermediates are assumed to be stabilized by the axial anionic ligands. The cysteine thiolate ligation at the axial site of the heme in cytochrome P-450 was originally proposed by an EPR study[7] and proved by resonance Raman (RR)[8] and X-ray crystallographic[9] studies. The proximal ligation of tyrosine phenolate in catalase was proved by X-ray crystallographic studies.[10] In the case of peroxidase, hydrogen bonding or deprotonation of proximal imidazole was suggested.[11] Therefore, the differences in the coordination nature of the proximal ligand are the essential factor for the reaction of heme enzymes.

The RR studies of cytochrome P-450[12] and its model complexes[13] have been reported previously. The thiolate iron(III) porphyrin complex, however, has not been fully characterized thus far, in part due to its inherent instability.[14] Though arene-[15] and alkanethiolate[16] complexes of iron porphyrin were prepared, these compounds were reported to be unstable in solution and to react immediately to give the μ-oxo dimer species upon exposure to air.[15b] In this work, we could successfully prepare the stable thiolate and phenolate complexes of (octaethylporphinato)iron(III), Fe(OEP),[17] that mimic the active site structure of the resting state of cytochrome P-450 and catalase, respectively. We studied the formation process and the electronic structure of these complexes by addition of a series of phenols, carboxylic acids (ROH), and thiols (RSH) to the Fe(OEP)(OMe) complex. The equilibrium constants for addition of ROH and the second-order rate constants for addition of RSH were measured by visible spectral techniques for the first time.

Materials and Methods

Titration with Phenols and Carboxylic Acids. The crystalline Fe(OEP)(OMe) complex was prepared as described.[18] The chloroform solution of Fe(OEP)Cl was vigorously shaken with aqueous KOH solution three times in a separatory funnel. The organic layer was evaporated and dissolved in chloroform, and methanol was allowed to diffuse slowly. Anal. Calcd for $FeC_{37}H_{47}N_4O$,[18] Fe(OEP)(OMe): C, 71.72; H, 7.65; N, 9.04. Found: C, 71.66; H, 7.42; N, 9.16.

Spectrophotometric measurements were made on a Shimadzu UV-2100 spectrophotometer. Visible spectra were obtained with ca. 0.1 mM Fe(OEP)(OMe)/methylene chloride (Nakarai Chemicals, SP Grade)

(1) (a) Nagoya City University. (b) University of Tokyo.
(2) Dawson, J. H. *Science* **1988**, *240*, 433.
(3) (a) Keilin, D.; Mann, T. *Proc. R. Soc. London, B* **1937**, *122*, 119. (b) Theorell, H. *Ark. Kemi, Mineral. Geol.* **1941**, *14B*, 1. (c) Chance, B. *J. Biol. Chem.* **1943**, *151*, 553. (d) Chance, B. *Arch. Biochem. Biophys.* **1952**, *24*, 410. (e) George, P. *Biochem. J.* **1953**, *54*, 267. (f) Yamazaki, I.; Mason, H. S.; Piette, L. H. *J. Biol. Chem.* **1960**, *235*, 2444.
(4) (a) Chance, B. *J. Biol. Chem.* **1952**, *194*, 471. (b) Jones, P.; Middlemiss, D. N. *Biochem. J.* **1972**, *130*, 411. (c) Palcic, M. M.; Dunford, H. B. *J. Biol. Chem.* **1980**, *255*, 6128.
(5) (a) Chance, B. *Arch. Biochem. Biophys.* **1952**, *41*, 404. (b) Theorell, H.; Ehrenberg, A. *Arch. Biochem. Biophys.* **1952**, *41*, 442. (c) Brill, A. S.; Williams, R. J. P. *Biochem. J.* **1961**, *78*, 253.
(6) Dolphin, D.; Forman, A.; Borg, D. C.; Fajer, J.; Felton, R. H. *Proc. Natl. Acad. Sci. U.S.A.* **1971**, *68*, 614.
(7) Murakami, K.; Mason, H. S. *J. Biol. Chem.* **1967**, *242*, 1102.
(8) Champion, P. M.; Stallard, B. R.; Wagner, G. C.; Gunsalus, I. C. *J. Am. Chem. Soc.* **1982**, *104*, 5469.
(9) (a) Poulos, T. L.; Finzel, B. C.; Gunsalus, I. C.; Wagner, G. C.; Kraut, J. *J. Biol. Chem.* **1985**, *260*, 16122. (b) Poulos, T. L.; Finzel, B. C.; Howard, A. J. *Biochemistry* **1986**, *25*, 5314. (c) Poulos, T. L.; Finzel, B. C.; Howard, A. J. *J. Mol. Biol.* **1987**, *195*, 687.
(10) (a) Reid, T. J., III; Murthy, M. R. N.; Sicignano, A.; Tanaka, N.; Musick, W. D. L.; Rossman, M. G. *Proc. Natl. Acad. Sci. U.S.A.* **1981**, *78*, 4767. (b) Murthy, M. R. N.; Reid, T. J., III; Sicignano, A.; Tanaka, N.; Rossman, M. G. *J. Mol. Biol.* **1981**, *152*, 465.
(11) (a) Peisach, J. *Ann. N.Y. Acad. Sci.* **1975**, *244*, 187. (b) Morrison, M.; Schonbaum, R. *Annu. Rev. Biochem.* **1976**, *45*, 861. (c) Teraoka, J.; Kitagawa, T. *J. Biol. Chem.* **1981**, *256*, 3969. (d) Quinn, R.; Mercer-Smith, J.; Burstyn, J. N.; Valentine, J. S. *J. Am. Chem. Soc.* **1984**, *106*, 4136.
(12) (a) Ozaki, Y.; Kitagawa, T.; Kyogoku, Y.; Shimada, H.; Iizuka, T.; Ishimura, Y. *J. Biochem. (Tokyo)* **1976**, *80*, 1447. (b) Ozaki, Y.; Kitagawa, T.; Kyogoku, Y.; Imai, Y.; Hashimoto-Yutsudo, C.; Sato, R. *Biochemistry* **1978**, *17*, 5826. (c) Champion, P. M.; Gunsalus, I. C. *J. Am. Chem. Soc.* **1977**, *99*, 2000. (d) Uno, T.; Nishimura, Y.; Makino, R.; Iizuka, T.; Ishimura, Y.; Tsuboi, M. *J. Biol. Chem.* **1985**, *260*, 2023. (e) Tsubaki, M.; Ichikawa, Y. *Biochim. Biophys. Acta* **1985**, *827*, 268. (f) Champion, P. M.; Gunsalus, I. C.; Wagner, G. C. *J. Am. Chem. Soc.* **1978**, *100*, 3743. (g) Bangcharoenpaurpong, O.; Champion, P. M.; Martinis, S. A.; Sligar, S. G. *J. Chem. Phys.* **1987**, *87*, 4273.
(13) (a) Chottard, G.; Schappacher, M.; Ricard, L.; Weiss, R. *Inorg. Chem.* **1984**, *23*, 4557. (b) Anzenbacher, P.; Sipal, Z.; Strauch, B.; Twardowski, J.; Proniewicz, L. M. *J. Am. Chem. Soc.* **1981**, *103*, 5928.
(14) Sakurai, H.; Shimomura, S.; Ishizu, K. *Chem. Pharm. Bull.* **1977**, *25*, 199.
(15) (a) Koch, S.; Tang, S. C.; Holm, R. H.; Frankel, R. B.; Ibers, J. A. *J. Am. Chem. Soc.* **1975**, *97*, 916. (b) Tang, S. C.; Koch, S.; Papaefthymiou, G. C.; Foner, S.; Frankel, R. B.; Ibers, J. A.; Holm, R. H. *J. Am. Chem. Soc.* **1976**, *98*, 2414.
(16) Ogoshi, H.; Sugimoto, H.; Yoshida, Z. *Tetrahedron Lett.* **1975**, 2289.
(17) Abbreviations used: OEP, dianion of octaethylporphyrin; PPIXDME, dianion of protoporphyrin IX dimethyl ester; TPP, dianion of tetraphenylporphyrin; TTOHP, dianion of 5-(2-hydroxyphenyl)-10,15,20-tritolylporphyrin; RR, resonance Raman; PhOH, phenol; PhSH, thiophenol; AcOH, acetic acid.
(18) Hatano, K.; Uno, T. *Bull. Chem. Soc. Jpn.*, in press.

0020-1669/90/1329-2803$02.50/0

Table I. Equilibrium Constants for Reactions of Fe(OEP)(OMe) with Phenols and Electronic Spectral Data for Products

phenols	pK_a	log K/M^{-1}	band IV[a]/nm	band III/nm	band I/nm
none[b]	15.5		467 (14.22)[c]	513 sh (8.12)	580 (9.77)
4-methylphenol	10.17	3.49	490 (12.74)	520 sh (10.95)	602 (8.85)
phenol	9.89	3.50	490 (12.21)	520 sh (10.77)	603 (8.23)
4-chlorophenol	9.18	4.35	492 (11.97)	523 sh (10.69)	607 (7.91)
4-cyanophenol	7.95	4.98	496 (11.51)	522 (10.95)	615 (6.74)
4-nitrophenol	7.15	5.15	497 (11.91)	524 (11.41)	618 (6.42)
2,4,6-trichlorophenol	6.00	5.23	501 (11.09)	528 (11.32)	620 (6.27)
2,5-dinitrophenol	5.15	4.90	499 (10.09)	529 (9.59)	625 (5.44)
2,4-dinitrophenol	3.96	4.93	500 (10.74)	530 (9.86)	629 (5.10)
2,4,6-trinitrophenol	0.38	>6	504 (10.24)	537 sh (8.67)	637 (3.83)

[a] See ref 25. [b] The data for Fe(OEP)(OMe). [c] The millimolar extinction coefficients are given in parentheses.

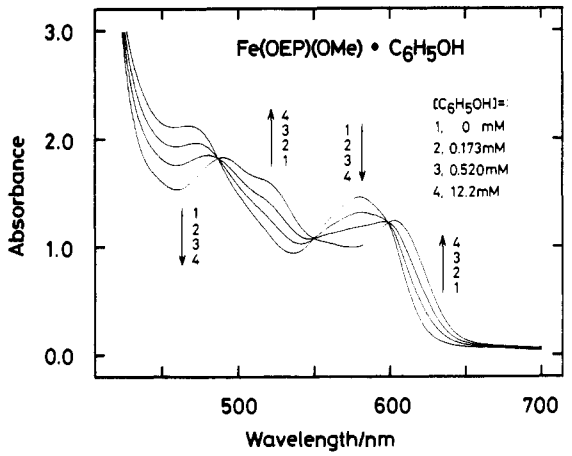

Figure 1. Visible spectral changes upon addition of phenol to Fe(OEP)(OMe). Aliquots of phenol solutions were added to 3 mL of 150 μM Fe(OEP)(OMe) in methylene chloride. Phenol concentrations (mM): (1) 0; (2) 0.173; (3) 0.520; (4) 12.2.

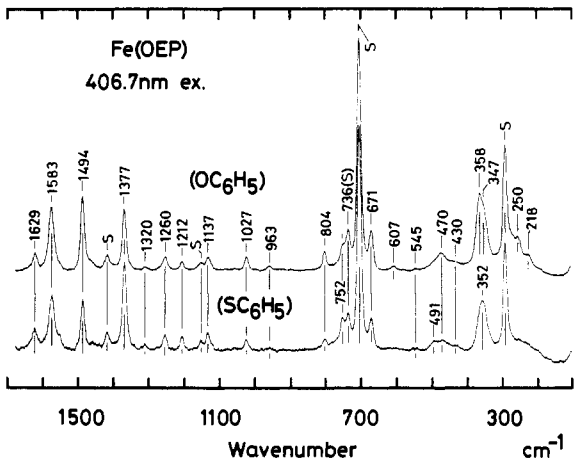

Figure 2. Resonance Raman spectra of Fe(OEP)(OPh) and Fe(OEP)(SPh): (upper) ca. 0.15 mM Fe(OEP)(OMe) dissolved in the solution of 30.3 mM phenol in methylene chloride; (lower) ca. 0.15 mM Fe(OEP)(OMe) dissolved in the solution of 1.0 mM thiophenol in methylene chloride. The lines marked with S denote those of the solvent. Raman scattering was excited with the 406.7-nm line. The slit width was 5 cm^{-1}.

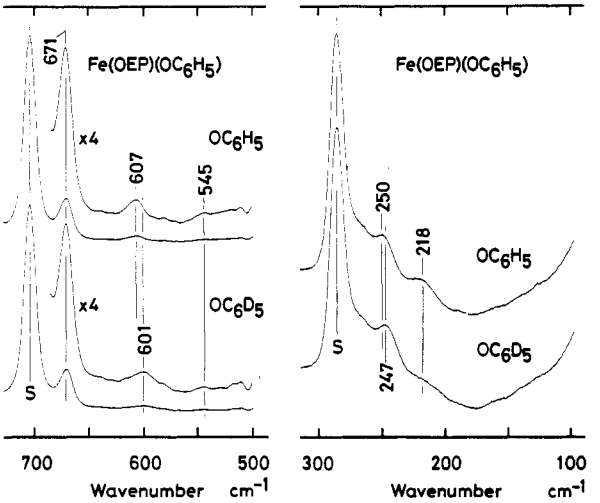

Figure 3. Effect of the substitution by isotope-labeled phenol on the resonance Raman spectrum of Fe(OEP)(OPh). The left panel is for the frequency region between 500 and 700 cm^{-1}, and the right panel, for that between 100 and 300 cm^{-1}. Solutions of ca. 0.15 mM Fe(OEP)(OMe) containing 30.3 mM C_6H_5OH (upper spectra) and C_6D_5OD (lower spectra) were used. Spectral conditions were the same as in Figure 2.

solution, to which aliquots of stock solutions of phenol or carboxylic acids had been added. The phenols and carboxylic acids used were of the purest grade available. The graphical procedure for obtaining the equilibrium constants is given in the Appendix.

Kinetic Trace of Thiol Reactions. The reactions of thiol derivatives with Fe(OEP)(OMe) were initiated by mixing the Fe(OEP)(OMe) solution and methylene chloride solutions containing an appropriate amount of thiol derivatives. The absorbance changes were monitored at 580 nm (see Figure 6) by the use of a Shimadzu UV-200S spectrophotometer equipped with a thermostated cell compartment attached to a circulating constant-temperature bath, which controlled the temperature at 20.0 ± 0.2 °C in the cell compartment.

RR Spectroscopy. RR spectra were obtained by using a detecting system as described previously.[19] The 406.7-nm line of a krypton ion laser (Spectra Physics, SP 164-01) was employed as an excitation source. Laser power at the sample was approximately 10 mW. A methylene chloride solution containing ca. 0.1 mM Fe(OEP)(OMe) and an appropriate amount of phenol or thiophenol was prepared. Perdeuterated phenol (98 atom % D, from Aldrich) was used for the isotopic shift experiments. The sample was spun in the rotating cell throughout the measurements to avoid local heating and to minimize the photoinduced decomposition. The spectral data were all transferred to a PDP11/23 DEC minicomputer and processed.

Results

Formation of the Phenolate Complex. In Figure 1 are shown the typical spectral changes in the visible region when phenol is added to Fe(OEP)(OMe). The isosbestic points are clearly observed at 484, 550, and 599 nm, indicating two spectral species in equilibrium. The absorption maxima and extinction coefficients for Fe(OEP)(OMe) and for the series of phenolate adducts are listed in Table I.

The formation of the five-coordinate ferric high-spin complex Fe(OEP)(OPh) was confirmed by RR spectroscopy.[20] In Figure 2 (upper) is shown the RR spectrum of the Fe(OEP)(OPh) complex. The ν_{10}, ν_2, ν_3, and ν_4 lines,[21] which are vibrations of

(19) (a) Makino, R.; Uno, T.; Nishimura, Y.; Iizuka, T.; Tsuboi, M.; Ishimura, Y. *J. Biol. Chem.* **1986**, *261*, 8376. (b) Uno, T.; Nishimura, Y.; Tsuboi, M.; Makino, R.; Iizuka, T.; Ishimura, Y. *J. Biol. Chem.* **1987**, *262*, 4549.

(20) (a) Spiro, T. G. *Iron Porphyrins*; Lever, A. B. P., Gray, H. B., Eds.; Addison-Wesley: Reading, MA, 1983; Part II, p 89. (b) Spiro, T. G. *Adv. Protein Chem.* **1985**, *37*, 111. (c) Asher, S. A. *Methods Enzymol.* **1981**, *76*, 371. (d) Felton, R. H.; Yu, N.-T. *The Porphyrins*; Dolphin, D., Ed.; Academic Press: New York, 1978; Vol. III, Part A, pp 347.

Table II. Equilibrium Constants for Reactions of Fe(OEP)(OMe) with Carboxylic Acids and Electronic Spectral Data for Products

carboxylic acids	pK_a	log K/M^{-1}	band IV[a]/nm	band III/nm	band I/nm
acetic acid	4.75	3.09	499 (9.44)[b]	529 (9.22)	623 (5.39)
benzoic acid	4.20	3.60	501 (9.20)	531 (9.32)	624 (5.41)
chloroacetic acid	2.87	4.76	502 (9.40)	531 (9.34)	629 (5.26)
dichloroacetic acid	1.30	~6	504 (9.19)	532 (8.85)	633 (4.73)
trichloroacetic acid	0.65	>6	505 (9.20)	532 (8.66)	635 (4.39)

[a] See ref 25. [b] The millimolar extinction coefficients are given in parentheses.

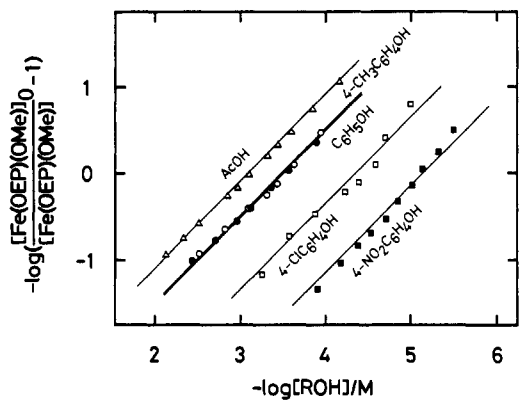

Figure 4. Analysis of absorbance data for the reactions of ROH derivatives with Fe(OEP)(OMe).

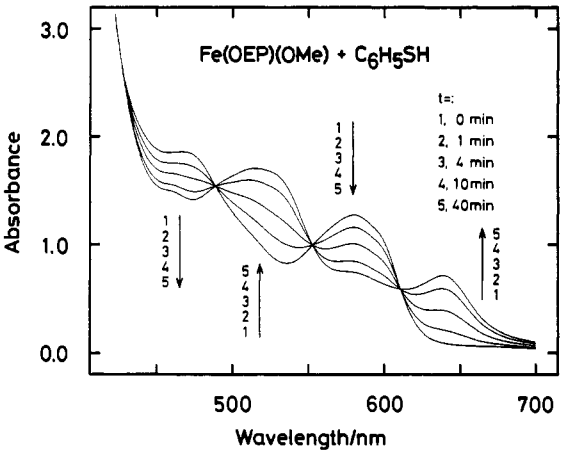

Figure 5. Visible spectral changes upon addition of thiophenol to Fe(OEP)(OMe). The solution of thiophenol (327 μM) was added to 130 μM Fe(OEP)(OMe) in methylene chloride at time zero. Time (min): (1) 0; (2) 1; (3) 4; (4) 10; (5) 40.

the porphyrin macrocycle, were observed at 1629, 1583, 1494, and 1377 cm^{-1}, respectively. The frequencies of these lines are quite similar to those of $[Fe(OEP)]_2O$[22] and Fe(OEP)Cl,[23] which are five-coordinate ferric high-spin complexes.

The spectral features of Fe(OEP)(OPh) also closely resemble those of Fe(OEP)(OMe). Instead of the Raman line at 541 cm^{-1}, which was assignable to the ν(Fe–OMe) stretch in Fe(OEP)(OMe),[24] a new line has appeared at 607 cm^{-1}. The 607-cm^{-1} line was sensitive to the phenol isotope substitution (Figure 3, left). The line shifted toward lower energy, with the mass of phenolate increasing from OC_6H_5 to OC_6D_5. The magnitude of the observed isotopic shift was in perfect agreement with that calculated for a stretching mode of the Fe–OPh molecule (6 cm^{-1}). In addition to the 607-cm^{-1} line, another isotope-sensitive line at 250 cm^{-1} for OC_6H_5, which downshifted to 247 cm^{-1} upon substitution by OC_6D_5 (Figure 3, right), has been noted. These phenol-isotope-sensitive lines will be discussed later.

Equilibrium Constant Evaluation. The absorbance changes at three to four wavelengths were used for the equilibrium constant evaluation for phenols and carboxylic acids (ROH). Typically, absorbance data at 467 and 580 nm and band III,[25] which appears around 520 nm, were taken from the spectral changes shown in Figure 1. The data of band I (603 nm in Figure 1) were used in some cases, if those were available. The equilibrium constants, K, were obtained graphically according to the Appendix. A typical analytical plot is shown in Figure 4. In every case of ROH utilized, the graph yields a straight line and the slope is unity. This indicates that 1 mol of ROH is involved in the reaction, even in high concentration of ROH.

The values of log K for phenol derivatives and carboxylic acids extrapolated from the intercept of the graph (e.g. Figure 4) are summarized in Tables I and II, respectively. The equilibrium constants for 2,4,6-trinitrophenol and di- and trichloroacetic acids were too large to evaluate precise log K values. The log K value is considered to be a function of the pK_a of the ROH derivatives, which is also tabulated. The phenol derivative having a bulky nitro group at position 2 of the phenol ring seems to give a log K value smaller than that expected from the steric effect (Table I).

The phenols and the carboxylic acids react similarly with Fe(OEP)(OMe). The ROH moieties that have small pK_a values promote the formation (large log K) of the product species, Fe(OEP)(OR). This behavior of ROH is contrary to that of neutral ligands such as imidazoles and pyridines, where those ligands with large pK_a values of their conjugate acids promote the bisligation of these bases to the iron porphyrin.[24,26]

Reactions of Thiols. In contrast to the phenols and carboxylic acids, thiols were found to react with Fe(OEP)(OMe) in an apparent irreversible manner (time dependent). The reaction of some thiol derivatives was slow enough to measure the kinetics of the formation of the product species at 20 °C. The addition of 1 equiv of a thiol derivative was sufficient to form the final product species in every case. In Figure 5 are shown typical spectral changes after the addition of thiophenol to Fe(OEP)(OMe). The absorption maxima of Fe(OEP)(OMe) diminished with a half-life of about 4 min, and a new species emerged that showed absorption maxima at 516 and 639 nm. However, the reaction of 4-nitrothiophenol was finished within the mixing time (less than 5 s), and the absorption maxima of the product species were shifted to 511 and 643 nm. The observed wavelengths coincide well with those reported for the thiolate complexes Fe(OEP)(SC_6H_5) and Fe(OEP)($SC_6H_4NO_2$).[15b] The RR spectrum of the Fe(OEP)(SPh) complex is shown in Figure 2 (lower). The RR spectral features are very close to those of Fe(OEP)(OPh), especially for the vibrations of the high-frequency modes. Therefore, the product is also a five-coordinate ferric high-spin complex, Fe(OEP)(SPh). In this spectrum, the 491-cm^{-1} line was apparent instead of the 607-cm^{-1} line for Fe(OEP)(OPh). This frequency is somewhat higher than that observed for the ν(Fe–S) stretching mode in cytochrome P-450cam (351 cm^{-1}).[8,12g]

(21) Abe, M.; Kitagawa, T.; Kyogoku, Y. *J. Chem. Phys.* **1978**, *69*, 4526.
(22) Callahan, P. M.; Babcock, G. T. *Biochemistry* **1981**, *20*, 952.
(23) Teraoka, J.; Hashimoto, S.; Sugimoto, H.; Mori, M.; Kitagawa, T. *J. Am. Chem. Soc.* **1987**, *109*, 180.
(24) Uno, T.; Hatano, K.; Nawa, T.; Nakamura, K.; Nishimura, Y.; Arata, Y. Manuscript in preparation.
(25) The notation of bands I–IV in the text is used to avoid confusion with RR lines. The notation is close to Falk's classic notation in wavelengths regardless of electronic characterization: Falk, J. E. *Porphyrins and Metalloporphyrins*; Elsevier: Amsterdam, 1964.
(26) (a) Walker, F. A.; Lo, M.-W.; Ree, M. T. *J. Am. Chem. Soc.* **1976**, *98*, 5552. (b) Yoshimura, T.; Ozaki, T. *Bull. Chem. Soc. Jpn.* **1979**, *52*, 2268.

Table III. Rate Constants for Formation of Fe(OEP)(SR) and Electronic Spectral Data for Products

thiols	pK_a	$k/M^{-1}\ s^{-1}$	band IV[a]/nm	band III/nm	band I/nm
n-butyl mercaptan	10.66	1.22	504 (12.47)[b]	534 sh (10.17)	623 (7.05)
benzyl mercaptan	9.43	0.91	505 (12.12)	533 sh (10.61)	627 (6.97)
methyl thioglycolate	7.8	2.67	506 (11.70)	531 (10.95)	633 (6.11)
thiophenol	6.54	10.6	516 (13.25)	527 sh (12.96)	639 (5.64)
4-fluorothiophenol	6.42	23.1	513 (13.34)	530 sh (12.79)	639 (5.58)
4-nitrothiophenol	5.08	>1000	511 (13.55)	538 sh (12.04)	643 (5.61)

[a] See ref 25. [b] The millimolar extinction coefficients are given in parentheses.

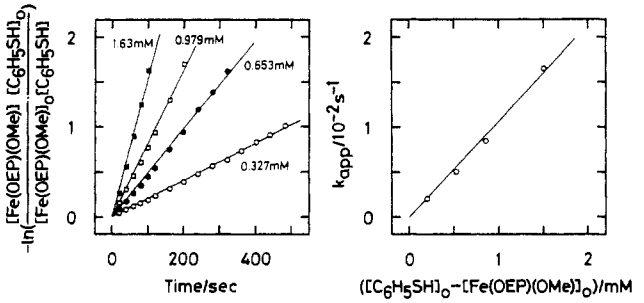

Figure 6. Analysis of absorbance data for the reaction of thiophenol with Fe(OEP)(OMe).

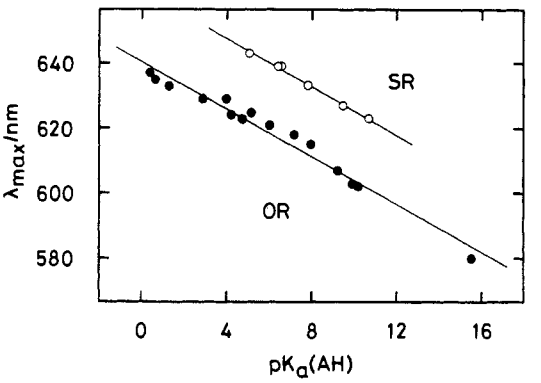

Figure 7. Correlation between pK_a values of the conjugate acid of the ligand and the wavelength maxima of band I.

As seen in Figure 5, the reaction of thiols (RSH) with Fe(OEP)(OMe) proceeds with one set of isosbestic points. Therefore, the reaction should be expressed as an apparent single step:

$$Fe(OEP)(OMe) + RSH \xrightarrow{k} Fe(OEP)(SR) + MeOH \quad (1)$$

The apparent rate constant, k_{app}, is given by

$$-\ln\left(\frac{[Fe(OEP)(OMe)]}{[Fe(OEP)(OMe)]_0}\frac{[RSH]_0}{[RSH]}\right) = k_{app}t \quad (2)$$

and is correlated with the second-order rate constant, k:

$$k_{app} = k([RSH]_0 - [Fe(OEP)(OMe)]_0) \quad (3)$$

The left term of eq 2 is plotted against time (t) in Figure 6 (left). The graph yielded zero intercept and a straight line in every case of [RSH] variation, the slope of which gives the value of k_{app}. The k_{app} values were replotted according to eq 3. The second-order kinetics is demonstrated by the linearity and zero intercept of the plots. The values of k, obtained from these procedures are summarized in Table III. The k value is clearly a function of the pK_a value of the thiol derivative utilized; the RSH with a small pK_a value reacts rapidly with Fe(OEP)(OMe).

Discussion

Coordination of Phenolate and Thiolate. An inverse linear correlation between the porphyrin core size and the porphyrin skeletal vibrations above 1450 cm^{-1} in RR spectra has been found.[27] As seen in Figure 2, the frequencies of these vibrations are in perfect agreement between Fe(OEP)(OPh) and Fe(OEP)(SPh) complexes, indicating that the core size of these species is the same. From the frequencies of the ν_{10} and ν_3 modes, Ct–N, the porphyrin center-to-pyrrole nitrogen distance, was calculated to be 2.01 ± 0.01 Å on the basis of the linear correlation. This value coincides well with that obtained from the X-ray crystallographic studies of Fe(PPIXDME)($SC_6H_4NO_2$) (2.017 Å),[15b] [Fe(TTOP)]$_2$ (2.016 Å),[28] and Fe(OEP)(picrate) (2.01 Å).[29]

In addition to the core-size markers, the oxidation state of the iron could be elucidated from the frequency of the ν_4 line.[20] This line was detected at 1377 cm^{-1} (Figure 2), indicating that iron is in the ferric state. It has been argued[15b] that the thiolate complexes of iron porphyrin are inherently unstable by virtue of the redox reaction

$$2Fe^{III}(P)(SR) \rightarrow 2Fe^{II}(P) + RSSR \qquad (P) = \text{porphyrin}$$

in which the initial event is presumably intramolecular reduction of Fe(III) by bound thiolate. The RR results show, however, that the reduction by thiolate ligands did not occur during the RR measurements.

In the Fe(OEP)(OPh) complex, we could detect two vibrations that were sensitive to the phenol isotope substitution (Figure 3). The higher frequency mode at 607 cm^{-1} is close to those proposed for the ν(Fe–O) stretching modes detected by 488.0-nm excitation in the abnormal hemoglobins, Hbs M Boston (603 cm^{-1})[30] and Iwate and Hyde Park (589 cm^{-1}),[30,31] all of which adopt the five-coordinate form with tyrosine as the only axial ligand. The frequency is somewhat higher than that of the ν(Fe–OMe) stretch (541 cm^{-1}).[24] This may in part be due to the coupling of the ν(Fe–OPh) stretching mode with phenolate ring vibrations. For iron cresolate compounds, this mode was assigned to the Fe–O stretch coupled appreciably with the phenolate ring vibrations.[32]

In addition to this ν(Fe–OPh) stretching mode, we have noticed that another Raman line at 250 cm^{-1} is sensitive to phenol isotope substitution. This line is not assignable to the phenolate ring vibrations nor to the phenolate ν(O–C) stretching mode because these vibrations of the heme-coordinated tyrosine have been detected around 1500–1600 cm^{-1} and around 1300 cm^{-1}, respectively, in abnormal hemoglobins.[30,31] Alternatively, the δ(Fe–O–O) bending mode was observed at 279 cm^{-1} in the O_2 adduct of iron(II) phthalocyanine.[33] The higher mass of the phenyl group than of the oxygen atom may result in the lower frequency, and this is not incompatible with the assignment that the 250-cm^{-1} line is the δ(Fe–O–Ph) bending mode.

Correlation between Absorption Maxima and pK_a Value. The electronic spectral data are summarized in Tables I–III, respectively. In some cases, band III is obscured and appears as a

(27) (a) Choi, S.; Spiro, T. G.; Langry, K. C.; Smith, K. M.; Budd, D. L.; La Mar, G. N. *J. Am. Chem. Soc.* **1982**, *104*, 4345. (b) Spaulding, L. D.; Chang, C. C.; Yu, N.-T.; Felton, R. H. *J. Am. Chem. Soc.* **1975**, *97*, 2517. (c) Huong, P. V.; Pommier, J.-C. *C. R. Seances Acad. Sci., Ser. C* **1977**, *285*, 519. (d) Scholler, D. M.; Hoffman, B. M. *J. Am. Chem. Soc.* **1979**, *101*, 1655.
(28) Goff, H. M.; Shimomura, E. T.; Lee, Y. J.; Scheidt, W. R. *Inorg. Chem.* **1984**, *23*, 315.
(29) Hatano, K.; Scheidt, W. R. Unpublished results.
(30) Nagai, K.; Kagimoto, T.; Hayashi, A.; Taketa, F.; Kitagawa, T. *Biochemistry* **1983**, *22*, 1305.
(31) Nagai, M.; Yoneyama, Y.; Kitagawa, T. *Biochemistry* **1989**, *28*, 2418.
(32) Pyrz, J. W.; Roe, A. L.; Stern, L. J.; Que, L., Jr. *J. Am. Chem. Soc.* **1985**, *107*, 614.
(33) Bajdor, K.; Oshio, H.; Nakamoto, K. *J. Am. Chem. Soc.* **1984**, *106*, 7273.

shoulder. The wavelengths of band I are clearly a function of pK_a. As shown in Figure 7, the wavelength maximum of band I is linearly correlated with the pK_a value of the acid (AH). The absorption band shift with respect to the pK_a of the anionic ligands has been pointed out earlier[34] for the π–π^* transitions in the five-coordinate Zn(TPP) complexes. The linear correlation observed (probably accidental) suggests the proportional free energy relationship of the ligand field with the pK_a of the anionic ligand.

Band I has been assigned to the porphyrin-to-iron $a_{1u}(\pi)$ and $a_{2u}(\pi) \rightarrow e_g(d_\pi)$ charge-transfer transitions.[35] Upon ligation of a strong-field ligand such as the methoxide anion, the greater charge donation by the coordinated methoxide will raise the d_π energy level of the iron. The fact that high-spin Fe(TPP)(OMe) spectra look rather like the spectra of low-spin complexes was explained[36] as a shifting of the allowed CT transition to higher energy compared with its value in Fe(TPP)(Cl). Since the electron-donating ability could be measured in terms of the pK_a value of a conjugate acid of a ligand, a strong ligand with a large pK_a value will raise the d_π energy level and hence will raise the CT transition energy.

In the case of Fe(OEP)(SR), another linear relationship, which nearly parallels the correlation in Fe(OEP)(OR), was found between the band I wavelength and pK_a value (Figure 7). The degrees of σ-donation should be essentially the same between the OR and SR ligands, which have pK_a values similar to those of the conjugate acids. Thus, the difference must be attributed largely to the difference in π-donation, which is negligible in the Fe(OEP)(OPh) case but significant for Fe(OEP)(SPh). The extra lone-pair electrons that reside in the 3p orbital of the sulfur atom will promote the electron π-donation into the iron d_π orbitals. An extended Hückel calculation on the first-row transition metals including Fe(III) indicated[35a] that the d_π orbitals are stabilized by the increase of d electrons, while the porphyrin π orbitals are less sensitive to the metal substitution. Therefore, migration of sulfur 3p electrons into d_π orbitals may stabilize the $e_g(d_\pi)$ orbitals and hence will reduce the CT transition energy. The similar concept of the p–d_π electron donation was introduced into the explanation of the low resonance Raman frequencies of the ν_4 mode[12a,b] and of the ν(Fe–CO) stretching mode[12d,e] in the ferrous and ferrous CO-ligated cytochrome P-450, respectively.

In conclusion, we could successfully trace the reaction of phenols, carboxylic acids, and thiols with the Fe(OEP)(OMe) complex. The derivative with a small pK_a value was found to promote the formation of the product species, which is a five-coordinate ferric high-spin complex, and to shift the absorption maxima of the product species to long wavelength. The reaction of the thiol derivatives differed from that of phenols and carboxylic acids such that the reaction was slow and was apparently irreversible. The p orbital of the sulfur atom was suggested to interact with, and to stabilize, the iron d_π orbitals. Such an effect of the sulfur p orbital may in part be related to the differences in the reactivities of cytochrome P-450 and catalase enzymes.

Acknowledgment. This work was supported, in part, by Grant-in-Aid 62771879 to T.U. from the Ministry of Education, Science, Culture of Japan.

Appendix

Graphical Evaluation of the Equilibrium Constant at Low Concentration of Ligand. The equilibrium reaction of Fe(OEP)(X) with n mol of ligand (L) is expressed as

$$\mathrm{Fe(OEP)(X)} + n\mathrm{L} \overset{K}{\rightleftharpoons} \mathrm{Fe(OEP)(L)}_n\mathrm{X} \qquad \text{(A1)}$$

$$K = [\mathrm{Fe(OEP)(L)}_n\mathrm{X}]/[\mathrm{Fe(OEP)(X)}][\mathrm{L}]^n \qquad \text{(A2)}$$

where K is the equilibrium constant. The initial concentration of Fe(OEP)(X), $[\mathrm{Fe(OEP)(X)}]_0$, is expressed as

$$[\mathrm{Fe(OEP)(X)}]_0 = [\mathrm{Fe(OEP)(L)}_n\mathrm{X}] + [\mathrm{Fe(OEP)(X)}] \qquad \text{(A3)}$$

Thus we obtain

$$K = \frac{[\mathrm{Fe(OEP)(X)}]_0 - [\mathrm{Fe(OEP)(X)}]}{[\mathrm{Fe(OEP)(X)}][\mathrm{L}]^n} \qquad \text{(A4)}$$

The logarithm of eq A4, after the rearrangement, gives

$$-\log\left(\frac{[\mathrm{Fe(OEP)(X)}]_0}{[\mathrm{Fe(OEP)(X)}]} - 1\right) = -\log K - n \log [\mathrm{L}] \qquad \text{(A5)}$$

The concentration of unreacted Fe(OEP)(X), [Fe(OEP)(X)], could be calculated from the following equation

$$[\mathrm{Fe(OEP)(X)}] = [\mathrm{Fe(OEP)(X)}]_0(A_c - A)/(A_c - A_0) \qquad \text{(A6)}$$

where A is the absorbance at the wavelength of interest, A_0 is the absorbance of Fe(OEP)(X) in the absence of L, and A_c is its absorbance in the presence of a large excess of L, sufficient to form the final product. Since the initial concentration of ligand, $[\mathrm{L}]_0$, is expressed as

$$[\mathrm{L}]_0 = [\mathrm{L}] + n[\mathrm{Fe(OEP)(L)}_n\mathrm{X}] \qquad \text{(A7)}$$

the concentration of free ligand, [L], after insertion of eq A3, could be calculated as

$$[\mathrm{L}] = [\mathrm{L}]_0 - n[\mathrm{Fe(OEP)(X)}]_0 + n[\mathrm{Fe(OEP)(X)}] \qquad \text{(A8)}$$

From eq A6 and A8, the plots of $-\log ([\mathrm{Fe(OEP)(X)}]_0/[\mathrm{Fe(OEP)(X)}] - 1)$ against $-\log [\mathrm{L}]$ are given as a straight line (eq A5), the slope of which is n and should be an integer. The values of $\log K$ are estimated from the intercept of the graph.

(34) Nappa, M.; Valentine, J. S. *J. Am. Chem. Soc.* **1978**, *100*, 5075.
(35) (a) Gouterman, M.; Hanson, L. K.; Khalil, G.-E.; Leenstra, W. R.; Buchler, J. W. *J. Chem. Phys.* **1975**, *62*, 2343. (b) Zerner, M.; Gouterman, M.; Kobayashi, H. *Theor. Chim. Acta* **1966**, *6*, 363. (c) Eaton, W. A.; Hochstrasser, R. M. *J. Chem. Phys.* **1968**, *49*, 985.
(36) (a) Kobayashi, H. *Adv. Biophys.* **1975**, *8*, 191. (b) Kobayashi, H.; Higuchi, T.; Kaizu, Y.; Osada, H.; Aoki, M. *Bull. Chem. Soc. Jpn.* **1975**, *48*, 3137.